Respecting Transfer Gap in Knowledge Distillation

Yulei Niu[*1] **Long Chen**[1] **Chang Zhou**[2] **Hanwang Zhang**[3]
[1]Columbia University [2]Damo Academy, Alibaba Group [3]Nanyang Technological University
{yn.yuleiniu,zjuchenlong}@gmail.com zhouchang.zc@alibaba-inc.com
hanwangzhang@ntu.edu.sg

Abstract

Knowledge distillation (KD) is essentially a process of transferring a teacher model's behavior, *e.g.*, network response, to a student model. The network response serves as additional supervision to formulate the machine domain (*machine* for short), which uses the data collected from the human domain (*human* for short) as a transfer set. Traditional KD methods hold an underlying assumption that the data collected in both human domain and machine domain are both independent and identically distributed (IID). We point out that this naïve assumption is unrealistic and there is indeed a transfer gap between the two domains. Although the gap offers the student model external knowledge from the machine domain, the imbalanced teacher knowledge would make us incorrectly estimate how much to transfer from teacher to student per sample on the non-IID transfer set. To tackle this challenge, we propose Inverse Probability Weighting Distillation (IPWD) that estimates the propensity score of a training sample belonging to the machine domain, and assigns its inverse amount to compensate for under-represented samples. Experiments on CIFAR-100 and ImageNet demonstrate the effectiveness of IPWD for both two-stage distillation and one-stage self-distillation.

1 Introduction

Knowledge distillation (KD) [21] transfers knowledge from a teacher model, *e.g.*, a big, cumbersome, and energy-inefficient network, to a student model, *e.g.*, a small, light, and energy-efficient network, to improve the performance of the student model. A common intuition is that a teacher with better performance will teach a stronger student. However, recent studies find that the teacher's accuracy is not a good indicator of the resultant student performance [8]. For example, a poorly-trained teacher with early stopping can still teach a better student [8, 11, 77]; or, a teacher with a smaller model size than the student is also a good teacher [77]; or, a teacher with the same architecture as the student helps to improve the student—self-distillation [13, 82, 81, 27].

Should we view KD in a perspective of domain transfer [12, 63], we would better understand the above counter-intuitive findings. From Figure 1, we can see that teacher predictions and ground-truth labels indeed behave differently. Although the teacher is trained on the balanced dataset, its predicted probability distribution over the dataset is imbalanced. Even on the same training set with the same model parameter, teachers with different temperature τ yield different "soft label" distributions from the ground-truth ones. This implies that human and teacher knowledge are from different domains, and there is a transfer gap that drives the "dark knowledge" [21] transferring from teacher to student—regardless of "strong" or "weak" teachers, it is a valid transfer as long as there is a gap. However, the transfer gap affects the distillation performance on the under-represented classes, *i.e.*, classes on the tail of teacher predictions, which is overlooked in recent studies. Take CIFAR-100 as an example. We rank and divide the 100 classes into 4 groups according to the ranks of predicted

[*]Work done when Yulei was at Nanyang Technological University.

36th Conference on Neural Information Processing Systems (NeurIPS 2022).

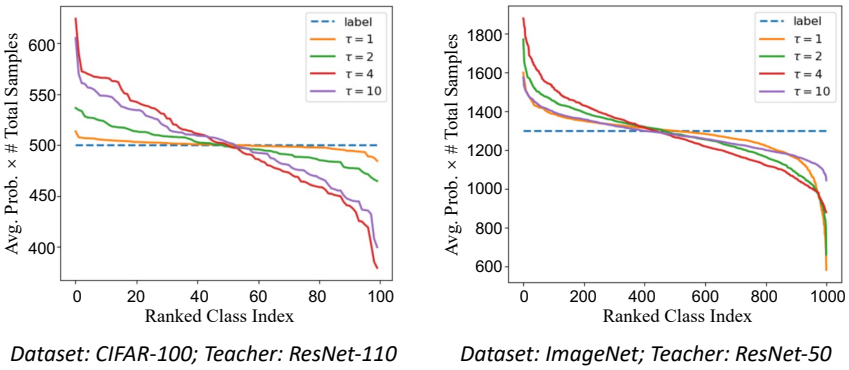

Figure 1: Illustration of the distribution discrepancies among ground-truth annotations and teacher predictions. Although the teacher model is trained on the balanced data (blue dashed), its prediction distributions are imbalanced according to various temperatures.

probability. As shown in Table 1, compared to vanilla training, KD achieves better performance in all the subgroups. However, the increase in the top 25 classes is much higher than that in the last 25 classes, *i.e.*, averagely 5.14% vs. 0.85%. We ask: what causes the gap from the first place; or more specifically, why does the teacher's non-uniform distributed predictions implies the gap? We answer in an *invariance vs. equivariance* learning point of view [4, 69]:

Human domain: context invariance. The discriminative generalization is the ability to learn both context-invariant and class-equivariant information from the diverse training samples per class. The human domain only provides context-invariant class-specific information, *i.e.*, hard targets. We normally collect a balanced dataset to formulate human domain.

Table 1: Improvement of KD over vanilla student for different classes. The metric is macro-average recall.

Arch. style	**Top 1-25**	**Top 26-50**	**Top 51-75**	**Top 76-100**
ResNet50 -> MobileNetV2	+4.96	+5.92	+1.76	+1.20
resnet32x4 -> ShuffleNetV1	+5.80	+2.68	+2.52	+0.84
resnet32x4 -> ShuffleNetV2	+4.72	+1.92	+2.24	+0.76
WRN-40-2 -> ShuffleNetV1	+5.08	+7.20	+4.48	+0.60

Machine domain: context equivariance. Teacher models often use a temperature variable to preserve the context. The temperature allows the teacher to represent a sample not only by its context-invariant class-specific information, but also its context-equivariant information. For example, a `dog` image with soft label 0.8·`dog` + 0.2·`wolf` may imply that the dog has wolf-like contextual attributes such as "fluffy coat" and "upright ears". Although the context-invariance (*i.e.*, class) is balanced in the training data, the context-equivariance (*i.e.*, context) is imbalanced because the context balance is not considered in class-specific data collection [67]. To construct the transfer set for the machine domain, the teacher model annotates each sample after seeing others, *i.e.*, being pre-trained on the whole set. Interestingly, the diverse context results in a long-tailed imbalanced distribution, which is exactly reflected in Figure 1. In other words, the teacher's knowledge is imbalanced even though the teacher is trained on a class-balanced dataset.

Now we are ready to point out how the transfer gap is not properly addressed in conventional KD methods. Conventional KD calculates the Cross-Entropy (CE) loss between the ground-truth label and student's prediction, and the Kullback–Leibler (KL) divergence [33] loss between the teacher's and student's predictions, where a constant weight is assigned for the two losses. This is essentially based on the underlying assumption that the data in both the human and machine domains are IID. Based on the analysis of context equivariance, we argue that the assumption is unrealistic, *i.e.*, *the teacher's knowledge is imbalanced*. Therefore, a constant sample weight for the KL loss would be a bottleneck. In this paper, we propose a simple yet effective method, Inverse Probability Weighting Distillation (IPWD), which compensates for the training samples that are under-weighted in the machine domain. For each training sample x, we first estimate its machine-domain propensity score $P(x|\textit{machine})$ by comparing class-aware and context-aware predictions. A sample with a low propensity score would have a high confidence from class-aware predictions and a low confidence from context-aware predictions. Then, IPWD assigns the inverse probability $1/P(x|\textit{machine})$ as the sample weight for the KL loss to highlight the under-represented samples. In this way, IPWD generates a pseudo-population [37, 26] to deal with the imbalanced knowledge.

We evaluate our proposed IPWD on two typical knowledge distillation settings: two-stage teacher-student distillation and one-stage self-distillation. Experiments conducted on CIFAR-100 [32] and ImageNet [10] demonstrate the effectiveness and generality of our IPWD.

Our contributions are three-fold:

- We formulate KD as a domain transfer problem and argue that the naïve IID assumption on machine domain neglects the imbalanced knowledge due to transfer gap.
- We propose Inverse Probability Weighting Distillation (IPWD) which compensate for the samples that are overlooked in the machine domain to tackle the imbalanced knowledge in transfer gap.
- Experiments on CIFAR-100 and ImageNet for both two-stage distillation and one-stage self-distillation show that the proper handling of the transfer gap is a promising direction in KD.

2 Related Work

Knowledge distillation (KD) was first introduced to transfer the knowledge from an effective but cumbersome model to a smaller and efficient model [21]. The knowledge can be formulated in either output space [21, 28, 35, 78, 77, 43, 61, 85, 31] or representation space [54, 25, 79, 30, 50, 19, 66, 7, 27]. KD has attracted a wide interest in theory, methodology, and applications [15]. For applications, KD has shown its great potential in various areas, including but not limited to classification [36, 53, 39, 23], detection [34, 59, 70], segmentation [18, 44, 38] for visual recognition tasks, and visual question answering [46, 1, 48], video captioning [49, 84], and text-to-image synthesis [64] for vision-language tasks. Recent studies further discussed how and why KD works. Specifically, Müller *et al.* [45] and Shen *et al.* [58] empirically analyzed the effect of label smoothing on KD. Cho *et al.* [8], Dong *et al.* [11], and Yuan *et al.* [77] pointed out that early stopping is a good regularization for a better teacher. Yuan *et al.* [77] further found that a poorly trained teacher, even a model smaller than the student, can improve the performance of the student. Besides, Memon *et al.* [41] and Zhou *et al.* [85] proposed a bias-variance trade-off perspective for KD. In this paper, we point out that existing KD methods hold an underlying assumption that the IID training samples are also IID in the machine domain, which overlooks the transfer gap.

Self-distillation is a special case of KD, which uses the student network itself as the teacher instead of the cumbersome model, *i.e.*, the teacher and student models have the same architecture [13, 82, 81, 27]. This process can be executed in iterations and produce a stronger ensemble model [13]. Similar to KD, traditional self-distillation follows a two-stage process: first pre-training a student model as the teacher, and then distilling the knowledge from the pre-trained model to a new student model. In order to perform the teacher-student optimization in one generation, recent studies [75, 31] proposed one-stage self-distillation that adopts student models at earlier epochs as teacher models. These one-stage self-distillation methods outperform vanilla students by large margins. In this paper, we also evaluate the effectiveness of our IPWD as a plug-in in one-stage self-distillation.

Inverse Probability Weighting (IPW) [55, 37, 26, 5], also known as inverse probability of treatment weighting or inverse propensity weighting, was proposed to correct the selection bias when the observations are non-IID. IPW uses the inverse of the probability (*i.e.*, propensity score) that the individual would be assigned to the treatment group to reweight the samples. Propensity-weighting techniques have been widely applied and studied in many areas [57], such as causal inference [26], complete-case analysis [37], machine learning [9, 6, 62], and recommendation systems [57, 72, 3]. In this paper, we view the distillation process as a domain transfer problem and adopt IPW to dynamically assign the weight to each training sample for the distillation loss.

3 Analysis

3.1 Knowledge Distillation (KD)

We view knowledge distillation from a perspective of domain transfer, and take the image classification task as the case study. Suppose that the training data $\mathcal{D} = \{\mathcal{X}, \mathcal{Y}\} = \{(x, y)\}$ contains x as the input (*e.g.*, image) and $y \in \mathbb{R}^C$ as its ground-truth annotation (*e.g.*, one-hot label), where C denotes the number of classes. A standard solution to train the classifier θ uses the cross-entropy loss as the

objective:

$$\mathcal{L}_{cls}(\textit{human};\theta) = \mathbb{E}_{(x,y)\sim P_{\textit{human}}}[\ell_{cls}(x,y;\theta)] \approx \frac{1}{|\mathcal{D}|}\sum_{(x,y)\in\mathcal{D}} \ell_{cls}(x,y;\theta) \triangleq \mathcal{L}_{cls}(\mathcal{D};\theta), \quad (1)$$

where $\ell_{cls}(x,y) = H(y^s, y)$ is the classification loss for sample x, $H(p,q) = \sum_{i=1}^{C} -q_i \log p_i$ denotes the cross entropy between p and q, $y^s = f(x;\theta)$ denotes the model's output probability given x, *i.e.*, $y^s_k = \frac{\exp(z^s_k)}{\sum_{i=1}^{C}\exp(z^s_i)}$, where z^s is the output logits of the model. The hard targets provide context-invariant class-specific information from the human domain. An assumption held behind Eq. (1) is that the samples are independent and identically distributed (IID) in the training and test set.

KD adopts a teacher model θ^t to generate soft targets as extra supervisions, *i.e.*, context-equivariant information. To formulate the machine domain, traditional KD methods commonly use the training set $\mathcal{D}$ to construct the transfer set $\mathcal{D}^t$ using the same copy of $\mathcal{X}$, *i.e.*, $\mathcal{D}^t = \{(x, y^t)\}$ where $y^t = f(x;\theta^t)$ and $x \in \mathcal{X}$. Traditional KD approaches use the KL divergence [33] loss for knowledge transfer:

$$\mathcal{L}_{dist}(\textit{machine};\theta) = \mathbb{E}_{(x,y)\sim P_{\textit{machine}}}[\ell_{dist}(x,y;\theta)] \approx \frac{1}{|\mathcal{D}^t|}\sum_{(x,y^t)\in\mathcal{D}^t} \ell_{dist}(x,y^t;\theta) \triangleq \mathcal{L}_{dist}(\mathcal{D}^t;\theta), \quad (2)$$

where $\ell_{dist}(x,y^t;\theta) = \tau^2 \cdot [H(y^s_\tau, y^t_\tau) - H(y^t_\tau, y^t_\tau)]$ denotes the distillation loss for sample x. Normally, the outputs of the student and teacher are softened using a temperature τ, *i.e.*, $y^s_{\tau,k} = \frac{\exp(z^s_k/\tau)}{\sum_{i=1}^{C}\exp(z^s_i/\tau)}$ and $y^t_{\tau,k} = \frac{\exp(z^t_k/\tau)}{\sum_{i=1}^{C}\exp(z^t_i/\tau)}$. The overall objective combines $\mathcal{L}_{cls}$ and $\mathcal{L}_{dist}$ as:

$$\mathcal{L}_{kd} = \alpha \cdot \mathcal{L}_{cls} + \beta \cdot \mathcal{L}_{dist}, \quad (3)$$

where α and β are the hyper-parameters. The underlying assumption of traditional KD behind Eq. (2) is that the transfer set $\mathcal{D}^t$ is an unbiased approximation of the machine domain. However, the observed long-tailed and temperature-sensitive distributions of teacher's predictions in Figure 1 rationally challenge this assumption. As a result, samples with lower $P(x|\textit{machine})$ are under-represented during the distillation process, which affects the unbiasedness of knowledge transfer. This analysis indicates that Eq. (2) is not optimal to utilize the teacher's imbalanced knowledge.

3.2 Transfer Gap in KD

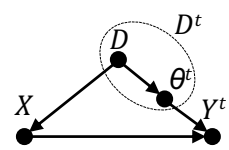

Figure 2: Causal graph for KD.

We interpret the transfer gap and its confounding effect from the perspective of causal inference. Figure 2 illustrates the causal relations between the image X, training data $\mathcal{D} = \{(x,y)\}$, teacher's parameters θ^t and teacher's output Y^t in KD. Overall, $\mathcal{D}$ and θ^t jointly act as the confounder of X and Y^t in the transfer set. First, the training set $\mathcal{D}$ and transfer set of teacher model $\mathcal{D}^t = \{(x, y^t)\}$ share the same image set, and $X = x$ is sampled from the image set of $\mathcal{D}$, i.e., $\mathcal{D}$ serves the cause of X. Second, the teacher θ^t is trained on $\mathcal{D}$, and y^t is calculated based on θ^t and x, i.e., $y^t = f(x;\theta^t)$. Therefore, X and θ^t are the cause of Y^t. Note that the transfer set is constructed based on the images on $\mathcal{D}$ and teacher model θ^t. Therefore, we regard the transfer set $\mathcal{D}^t$, the joint of $\mathcal{D}$ and θ^t, as the confounder of X and Y^t.

Although $\mathcal{D}$ is balanced when considering the context-invariant class-specific information, the context information (e.g., attributes) is overlooked, which makes the $\mathcal{D}$ imbalanced on context. As shown in Figure 1, such imbalanced context leads to an imbalanced transfer set $\mathcal{D}^t$ and further affects the distillation performance of teacher's knowledge.

To overcome such confounding effect, a commonly used technique is intervention via $P(y^t|do(x))$ instead of $P(y^t|x)$, which is formulated as $P(y^t|do(x)) = \sum_{\mathcal{D}^t} P(y|x,\mathcal{D}^t)P(\mathcal{D}^t) = \sum_{\mathcal{D}^t} \frac{P(x,y^t,\mathcal{D}^t)}{P(x|\mathcal{D}^t)}$. This transformation suggests that we can use the inverse of propensity score, $1/P(x|\mathcal{D}^t)$, as sample weight to implement the intervention and overcome the confounding effect. Thanks to the causality-based theory [55, 5], we can use the Inverse Probability Weighting (IPW) technique to overcome the confounding effect brought by the transfer gap.

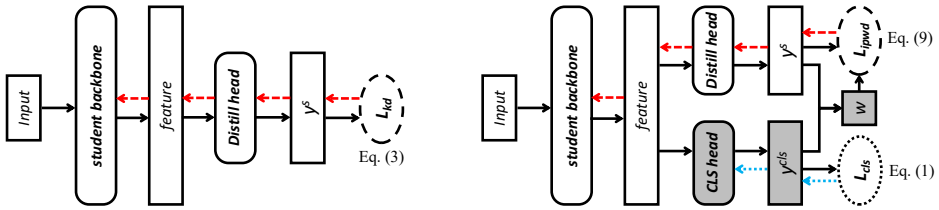

(a) Traditional KD (b) IPWD

Figure 3: The comparison of training pipelines between traditional KD and our IPWD. The module and outputs in grey are not used in the delivered student model.

4 Method

We propose a simple yet effective method, Inverse Probability Weighting Distillation (IPWD), to respect the transfer gap and imbalance knowledge in KD. In this section, we first introduce the overall framework of IPWD, then present the implementation details.

4.1 Inverse Probability Weighting for KD

As analyzed in Section 3, the IID training samples in the human domain are no longer IID in the machine domain. Simply assuming the training set as the perfect transfer set may lead to the selection bias: samples that match "head" knowledge are over-represented and easy to be observed, while samples that match "tail" knowledge are under-represented and hard to be observed. This would suppress the transfer of "tail" knowledge. The analysis from the perspective of causal inference in Section 3.2 suggests that we can use Inverse Probability Weighting (IPW) for debiased distillation. In short, IPW generates a pseudo-population where under-represented samples are assigned with large weights and over-represented samples are assigned with small weights. The weight for sample x is determined as the inverse of its probability, also known as propensity score, to the domain $d \in \{\textit{human}, \textit{machine}\}$, *i.e.*, $w_{x|d} = 1/p(x|d)$. We adopt IPW to KD and obtain the following objective for sample x:

$$\ell(x;\theta) = \sum_d w_{x|d} \cdot \ell_d(x, y^d; \theta) = \frac{1}{P(x|\textit{human})}\ell_{cls}(x, y; \theta) + \frac{1}{P(x|\textit{machine})}\ell_{dist}(x, y^t; \theta). \quad (4)$$

4.2 Implementation

Since the training and test data are normally IID in the human domain, we safely and rationally use the empirical risk. Therefore, we assign a constant weight to each sample when calculating the classification loss. For sure, the training and test samples can be both non-IID, *e.g.*, long-tailed recognition tasks, which is out of the scope of this paper.

As analyzed in Section 1, the assumption held by traditional KD, *i.e.*, both $P(X|\textit{human})$ and $P(X|\textit{machine})$ are IID, is unrealistic in practice. Therefore, we should consider the propensity score $P(x|\textit{machine})$ as a sample-specific value for the distillation loss to improve the generalization. Traditional IPW estimates the propensity score using logistic regression, *i.e.*, $\hat{P}(x|\textit{machine}) = 1/(1+\exp(-z_x))$, where z_x is the logit for x. Since the ground-truth annotation of $P(x|\textit{machine})$ is not available, it is not practicable to directly train the regression model in a fully-supervised manner. Therefore, we estimate the propensity score in an unsupervised way.

Recall that the samples with high propensity are over-represented in the transfer set. As a result, the student model would learn less from the under-represented group via distillation. Therefore, we use a classification-trained (CLS-trained) classifier for the human domain as reference, and assume that a KD-trained classifier for the machine domain is more confident for the over-represented group than the CLS-trained classifier. We compare the outputs of two classifiers to identify whether a sample is under-represented in the machine domain. Suppose that the KD-trained output is y^{kd} and the CLS-trained output is y^{cls}. The assumption implies that the logit z_x is negatively correlated with

(a) (b) (c)

Figure 4: Illustration of the sample weights. **Bold underlined class** denotes the ground-truth label. The areas in y^{kd} and y^{cls} represent the proportion of the predicted probability. A high rank indicates a large sample weight, while a low rank indicates a small sample weight.

$H(y^{kd}, y)$ and positively correlated with $H(y^{cls}, y)$, where $H(\cdot, \cdot)$ is the cross-entropy defined in Section 3. Considering the range of logit, we estimate z_x as $z_x = \log \frac{H(y^{cls},y)}{H(y^{kd},y)}$.

Figure 3 illustrates the comparison between traditional KD and our IPWD. We take the KD-trained student's output y^s as y^{kd}, and train an extra classifier head (*i.e.*, "CLS head" in Figure 3(b)) to calculate y^{cls}, which is optimized using the cross-entropy loss $\mathcal{L}_{cls}$ with the ground-truth labels. As shown in Table 5, we empirically found that directly using y^s and y^{cls} would lead to a high variance. For example, a wrongly classified sample may have a extremely large loss and heavily suppress the distillation of other samples. Therefore, we normalize the logits by dividing them by the standard deviation σ^s and σ^{cls}, *i.e.*, $\widetilde{y}^s = \frac{\exp(z_k^s/\sigma^s)}{\sum_{i=1}^{C}\exp\left(z_i^s/\sigma^s\right)}$ and $\widetilde{y}^{cls} = \frac{\exp\left(z_k^{cls}/\sigma^{cls}\right)}{\sum_{i=1}^{C}\exp\left(z_i^{cls}/\sigma^{cls}\right)}$. In this way, the outputs are at the same scale with a standard deviation equal to 1, which helps to reduce the variance. We finally take $\widetilde{y}^s$ as y^{kd} and $\widetilde{y}^{cls}$ as y^{cls}. Combining z_x into the propensity score, we have:

$$\hat{P}(x|\textit{machine}) = \frac{H(y^{cls}, y)}{H(y^{cls}, y) + H(y^{kd}, y)}, \tag{5}$$

and the estimated weight $\hat{w}_x$ for sample x is $\hat{w}_x = \frac{1}{\hat{P}(x|\textit{machine})} = 1 + \frac{H(y^{kd},y)}{H(y^{cls},y)}$. Figure 4 illustrates some examples of training samples and their assigned weights. Under-represented samples, for which the KD-trained classifier is less confident than the CLS-trained classifier, are assigned with a large weight (Figure 4(a)). Over-represented samples, for which the KD-trained classifier is more confident than the CLS-trained classifier, are assigned with a small weight (Figure 4(c)). Samples for which the two classifiers behave similarly are assigned with a balanced weight (Figure 4(b)). The weighted distillation loss is formulated as:

$$\mathcal{L}_{ipw\text{-}dist} = \frac{1}{|\mathcal{D}^t|} \sum_{(x,y^t)\in\mathcal{D}^t} \widetilde{w}_x \cdot \ell_{dist}(x, y^t; \theta), \tag{6}$$

Our final IPWD objective is formulated as:

$$\mathcal{L}_{ipwd} = \mathcal{L}_{cls} + \alpha\mathcal{L}_{ipw\text{-}dist} \tag{7}$$

where α is a trade-off hyper-parameter between classification and distillation.

Limitations and negative societal impacts.. As introduced in Section 4.2, we estimate the propensity score by comparing the heads of the student model. Therefore, the estimation relies on the quality of the student model. A poor student may not correctly estimate the propensity, which may further suppress the effectiveness of IPWD. Also, we hold an assumption that the training and test samples are IID in the human domain, which may not be valid for long-tailed tasks. To the best of our knowledge, as our work is purely an algorithm for knowledge distillation, we haven't found any negative societal impact.

Table 2: Top-1 accuracies (%) on CIFAR-100 for two-stage distillation. * denotes our reproduced results using the same teacher model.

	Same architecture style				Different architecture style			
Teacher Student	WRN-40-2 WRN-40-1	resnet56 resnet20	resnet110 resnet32	resnet32x4 resnet8x4	resnet32x4 ShuffleNetV1	WRN-40-2 ShuffleNetV1	ResNet50 vgg8	ResNet50 MobileNetV2
Teacher	75.61	72.34	74.31	79.42	79.42	75.61	79.34	79.34
Student	71.98	69.06	71.14	72.50	70.50	70.50	70.36	64.60
FitNet [54]	72.24	69.06	71.06	73.50	73.59	73.73	70.69	63.16
AT [79]	72.77	69.21	72.31	73.44	71.73	73.32	71.84	58.58
SP [68]	72.43	69.67	72.69	72.94	73.48	74.52	73.34	68.08
CC [52]	72.21	69.63	71.48	72.97	71.14	71.38	70.25	65.43
VID [2]	73.30	70.38	72.61	73.09	73.38	73.61	70.30	67.57
RKD [50]	72.22	69.61	71.82	71.90	72.28	72.21	71.50	64.43
PKT [51]	73.45	70.34	72.61	73.64	74.10	73.89	73.01	66.52
AB [20]	72.38	69.47	70.98	73.17	73.55	73.34	70.65	67.20
FT [30]	71.59	69.84	72.37	72.86	71.75	72.03	70.29	60.99
NST [25]	72.24	69.60	71.96	73.30	74.12	74.89	71.28	64.96
KD [21]	73.54	70.66	73.08	73.33	74.07	74.83	73.81	67.35
CRD [66]	74.14	71.16	73.48	75.51	75.11	76.05	74.30	69.11
WSLD* [85]	73.74	**71.53**	73.36	74.79	75.09	75.23	73.80	68.79
IPWD	**74.64**	71.32	**73.91**	**76.03**	**76.03**	**76.44**	**74.97**	**70.25**

5 Experiments

We take the image classification task as a case study to evaluate the effectiveness and generalizability of our IPWD. Following previous works [66, 85, 31], we conduct experiments with two settings, two-stage distillation and one-stage self-distillation.

5.1 Datasets and Settings

Datasets. We conducted experiments on CIFAR-100 [32] and ImageNet [10]. CIFAR-100 contains 50K images in the training set and 10K images in the test set from 100 classes. ImageNet provides 1.2M images in the training set and 50K images in the validation set from 1K classes.

Settings. Two-stage distillation is the conventional setting that pre-trains a teacher model at the first stage and transfers the knowledge to a student model at the second stage. Commonly, the teacher is a larger model, and the student is a smaller model. For self-distillation, the teacher and student have the same architecture. One-stage self-distillation aims to complete the teacher-student optimization simultaneously [75, 31], *i.e.*, the pre-training and transfer processes are reduced to one.

5.2 Two-stage Distillation

Baseline methods. For two-stage distillation, following Tian *et al.* [66] and Zhou *et al.* [85], we considered the following methods as baselines: KD [21], FitNet [54], AT [79], SP [68], CC [52], VID [2], RKD [50], PKT [51], FSP [76], AB [20], FT [30], NST [25], CRD [66], SSKD [74], and WSLD [85]. In particular, WSLD [85] is the most related work to us, which proposed a bias-variance trade-off perspective for KD and also assigns different weights to each training sample. Similarly, the weight is positive related to the cross-entropy loss of student's output. The main differences between our IPWD and WSLD are as follows. First, our formulation of samples weights is theoretically guaranteed by the causal theory behind Inverse Probability Weighting (IPW) [55, 37, 26, 5]. Second, WSLD estimates the sample weight using both the student model and the teacher model. As a comparison, we use the student model with two different classifier heads to guarantee that the capacities of the compared models are close.

Implementation. For experiments on CIFAR-100, we followed CRD [66] based on the open-sourced code. We set the trade-off hyper-parameter $\alpha = 5$ in Eq. (7) and the temperature $\tau = 10$. Other training details were the same as CRD [66] and provided in the appendix. For ImageNet, we followed

Table 3: Top-1 accuracies (%) on CIFAR-100 test set as a plug-in on SSKD [74]. We reproduced the results of SSKD using the same teacher model.

	Same architecture style				Different architecture style			
Teacher Student	WRN-40-2 WRN-16-2	WRN-40-2 WRN-40-1	resnet56 resnet20	resnet32x4 resnet8x4	ResNet50 MobileNetV2	resnet32x4 ShuffleNetV1	WRN-40-2 ShuffleNetV1	vgg13 MobileNetV2
Teacher	76.46	76.46	73.44	79.63	79.10	79.63	76.46	75.38
Student	73.64	72.24	69.63	72.51	65.79	70.77	70.77	65.79
SSKD* [74]	75.74	75.59	70.61	75.80	72.22	77.71	78.49	77.32
+ IPWD	**76.39**	**76.09**	**71.69**	**76.74**	**72.85**	**78.30**	**79.17**	**77.95**

Zhou *et al.* [85] to conduct experiments based on their open-sourced code. We used the same hyper parameters as WSLD [85], *i.e.*, α as 2.5 and τ as 2.

Comparison with baseline methods. Table 2 shows the results of student models on CIFAR-100 with different teacher-student architectures, which can be grouped into same architecture style and different architecture style. Note that the results of WSLD reported in [85] used a different pre-trained teacher model. Since some training techniques like early-stopping [8, 11, 77] may improve the distillation performance, we reimplemented WSLD using the same teacher model for a fair comparison. Overall, our IPWD outperforms KD by large margins and outperforms other baseline methods on most of the architectures, which demonstrates the effectiveness of our IPWD. In particular, the improvement with the same architecture style is smaller than the different style. The reason is that the different architecture style reflects the bigger gap between the human domain and machine domain. Since our IPWD weights the training samples to address the non-IID problem, IPWD successfully outperforms KD and other state-of-the-art methods by large margins when the transfer gap is significant.

Note that SSKD [74] achieves higher performance because of (1) a better teacher model, and (2) data augmentation for structured knowledge distillation. We further apply IPWD to SSKD as a plug-in by weighting the logit distillation objective and keeping the structured knowledge distillation terms unchanged. Table 3 shows that our IPWD can consistently improve SSKD by 0.5~1.0% for different architectures. These results indicate that our IPWD is a good complementary to distillation methods.

Table 4: Acc. (%) on ImageNet for two-stage distillation.

	Same arch. style		Diff. arch. style	
Teacher Student	ResNet-34 ResNet-18		ResNet-50 MobileNet-v1	
	Top-1	**Top-5**	**Top-1**	**Top-5**
Teacher	73.31	91.42	76.16	92.87
Student	69.75	89.07	68.87	88.76
AT [79]	71.03	90.04	70.18	89.68
NST [25]	70.29	89.53	—	—
FT [30]	—	—	69.88	89.50
FSP [76]	70.58	89.61	—	—
AB [20]	—	—	68.89	88.71
RKD [50]	70.40	89.78	68.50	88.32
KD [21]	70.67	90.04	70.49	89.92
Overhaul [19]	71.03	90.15	71.33	90.33
CRD [66]	71.17	90.13	69.07	88.94
SSKD [74]	71.62	90.67	—	—
DGKD [61]	71.73	**90.82**	—	—
WSLD [85]	**72.04**	90.70	71.52	90.34
IPWD	71.88	90.50	**72.65**	**91.08**

Table 4 further shows the comparison on ImageNet. Following CRD [66] and WSLD [85], we used two teacher-student architectures as the representatives. For the same architecture style, our IPWD improves KD by 1.21%, and achieves competitive performance compared to WSLD. For the different architecture style, the improvement of WSLD over KD drops from 1.37% to 1.03%. As a comparison, our IPWD improves KD by 2.16%, and outperforms WSLD by 1.13%. This improvement on the large-scale dataset further demonstrates the effectiveness of our IPWD to bridge the transfer gap when the student and teacher model have different architecture styles, which is more practical in real-world applications.

Ablation study: technical designs. As introduced in Section 4.2, we used an extra classifier head to produce CLS-trained output, and normalized the logits to reduce the variance for propensity estimation. Note that WSLD [85] uses the teacher model to estimate the sample weight, and the teacher model is also trained with the cross-entropy loss. Therefore, we considered an alternative that which replaces the classification head with the teacher model to produce the classification-aware

Table 5: Ablation study of technical designs for weight estimation on CIFAR-100. "CLS head" denotes the usage of an extra classification head. "logits norm." denotes that the logits are normalized before calculating the propensity.

			Same architecture style			Different architecture style		
			WRN-40-2 ↓ WRN-40-1	resnet110 ↓ resnet32	resnet32x4 ↓ resnet8x4	resnet32x4 ↓ ShuffleNetV1	resnet32x4 ↓ ShuffleNetV2	WRN-40-2 ↓ ShuffleNetV1
	CLS head	logits norm.						
			training diverges			52.81	57.99	53.31
		✓	74.01	73.41	75.89	75.49	76.48	76.34
	✓		74.42	73.48	75.97	75.80	76.45	75.96
IPWD	✓	✓	**74.64**	**73.91**	**76.03**	**76.03**	**76.61**	**76.61**

Table 6: Results on CIFAR-100 test set for the one-stage self distillation setting over four architectures. Top-1 and Top-5 indicate the accuracy.

Method	**Top-1**	**Top-5**	**ECE**	**AURC**	**Method**	**Top-1**	**Top-5**	**ECE**	**AURC**
ResNet-18	75.82	93.10	11.84	67.65	DenseNet-121	79.95	95.01	7.34	52.21
+ LS	79.06	93.98	10.79	57.74	+ LS	80.20	94.54	**0.92**	91.06
+ CS-KD [78]	78.70	94.30	6.24	56.56	+ CS-KD [78]	79.53	93.79	13.80	73.37
+ TF-KD [77]	77.12	93.99	11.96	61.77	+ TF-KD [77]	80.12	94.90	7.33	69.23
+ PS-KD [31]	79.18	94.90	1.77	52.10	+ PS-KD [31]	81.27	**96.10**	3.71	45.55
+ PS-KD + Ours	**79.82**	**95.15**	**1.39**	**49.71**	**+ PS-KD + Ours**	**81.60**	96.04	3.48	**45.33**
ResNet-101	79.25	94.72	10.02	55.45	ResNeXt-29	81.35	95.53	**4.17**	44.27
+ LS	80.16	94.93	3.43	95.76	+ LS	82.40	95.77	22.14	41.92
+ CS-KD [78]	79.24	94.38	12.18	64.44	+ CS-KD [78]	81.74	95.63	5.95	42.11
+ TF-KD [77]	79.90	94.90	6.14	58.80	+ TF-KD [77]	82.67	96.13	6.73	40.34
+ PS-KD [31]	80.57	95.70	6.92	49.01	+ PS-KD [31]	82.72	96.40	9.15	39.78
+ PS-KD + Ours	**81.39**	**95.91**	**3.19**	**43.82**	**+ PS-KD + Ours**	**83.30**	**96.60**	4.93	**37.49**

output. To evaluate the contribution of logits normalization, we considered an alternative that the logits are not normalized by the standard deviation. Results in Table 5 verify the contribution of each design. Without the classification head and logit normalization, the training is hard to converge or the performance is much worse. As a comparison, either the classification head or logit normalization helps with stable training. Besides, a combination of both further improves the performance and achieves the best results. The crash of training is due to the high variance of sample weights. Since the teacher model is well pre-trained and has more parameters, it has a larger capacity than the student model. Differently, an extra head with a shared backbone guarantees a similar capacity. Also, the normalization will avoid an extremely large or small CE loss, which further reduces the variance.

Teacher trained with label smoothing. Recent works [45, 58] observed that KD performs poorly with label smoothing. Similar to KD, the performance of IPWD drops when the teacher model is trained with label smoothing, but still outperforms KD. However, we found that the improvement of IPWD compared to KD also decreases with label smoothing. For example, on CIFAR-100, given ResNet50 as teacher and MobileNetV2 as student, IPWD outperforms KD by 1.12% (69.67% vs. 68.55%) without label smoothing, but the improvements drops to 0.56% (66.79% vs. 66.23%) with label smoothing. Given resnet32x4 as teacher and ShuffleNetV1 as student, IPWD outperforms KD by 1.52% (75.79% vs. 74.27%) without label smoothing, but the improvement drops to 0.53% (73.27% vs. 72.74%) with label smoothing. We observed that teacher trained with label smoothing produces more balanced predictions compared to teacher trained without label smoothing. Therefore, the results are consistent with our hypothesis that IPWD helps to bridge the transfer gap especially when the context information of teacher is imbalanced.

5.3 One-stage Self-Distillation

Baseline methods and metrics. For one-stage self-distillation, we apply our method to the state-of-the-art PS-KD [31] method as a plug-in, and consider label smoothing (LS) method and two self-distillation methods, CS-KD [78] and TF-KD [77], as baselines. PS-KD proposed a one-stage

framework that progressively distills the knowledge of a model itself to soften the one-hot supervisions as regularization. The knowledge is transferred using a conventional distillation loss. As for metrics, besides top-1 and top-5 accuracy, we follow Kim *et al.* [31] to report expected calibration error (ECE, %) and the area under the risk-coverage curve (AURC, $\times 10^3$). A low ECE indicates well-calibrated predictions, and a low AURC represents the well-separation of correct and incorrect predictions.

Implementation. We follow all the training details of PS-KD for a fair comparison. Specifically, the architectures we considered are ResNet-18 [17], ResNet-101 [16], ResNeXt-29 [73] (cardinality=8, width=64), and DenseNet-121 [24] (growth rate=32). During training, PS-KD gradually determine how much the student learns from the teacher's knowledge. The formulation is:

$$\mathcal{L}_{ps\text{-}kd} = (1 - \alpha_t) \cdot \mathcal{L}_{cls} + \alpha_t \cdot \mathcal{L}_{dist}, \tag{8}$$

where the trade-off parameter $\alpha_t = \alpha_T \times t/T$, T is the number of total epochs (*e.g.*, 300), t is the current epoch, and α_T is a hyperparameter. Compared to Eq. (8), our IPWD applied on PS-KD is formulated as

$$\mathcal{L}_{ps\text{-}kd+ipw} = (1 - \alpha_t) \cdot \mathcal{L}_{cls} + \alpha_t \cdot \mathcal{L}_{ipw\text{-}dist} \tag{9}$$

Since both the student and teacher models are poor at early epochs, the weight estimation is not accurate at early epochs, which may lead to a worse self-teacher. Therefore, we apply IPWD at the last 75 epochs over the total 300 epochs.

Comparison with baseline methods. Table 6 shows the results of one-stage self-distillation methods over four architectures. Our IPWD can effectively and constantly improve the top-1 accuracy of PS-KD by 0.33%∼0.82% with different architectures. Besides, our IPWD siginifantly lowers the ECE and AURC of PS-KD. These results demonstrate the effectiveness of our IPWD.

Ablation study: IPWD stage. We conduct an ablation study to analyze whether IPWD should be started from an early stage (*e.g.*, the beginning of training) or a late stage (*e.g.*, last 1/4 of the epochs). We take ResNeXt-29 as an example. As shown in Table 7, applying IPWD from the beginning slightly outperforms PS-KD and under-performs the student modal that applies IPWD only at the late stage by large margins. As the student model is poorly trained at the early stage, the weight estimation is inaccurate and hurts the performance of self-teacher. These results indicate that the quality of estimated weight and distillation performance relies on the student model and self-teacher.

Table 7: Ablation study on the start of applying IPWD.

Method	Top-1 Acc	Top-5 Acc	ECE	AURC
PS-KD [31]	82.72	96.40	9.15	39.78
+ IPWD (early)	82.86	96.35	8.56	38.16
+ IPWD (late)	**83.30**	**96.60**	**4.93**	**37.49**

6 Conclusion

In this paper, we we point out that conventional KD methods hold an invalid IID assumption and does not properly address the transfer gap between the context-invariant human domain and the context-equivariant machine domain, especially the imbalance knowledge of the teacher model on the transfer set. We further proposed a simple yet effective method, Inverse Probability Weighting Distillation (IPWD), to deal with the imbalanced knowledge caused by transfer gap. In the future, we will extend our IPWD to (1) tasks beyond classification, like detection and segmentation, and (2) long-tailed tasks where the training samples in the human domain are also non-IID.

Acknowledgement

We thank anonymous ACs and reviewers for their valuable discussion and insightful suggestions. This research is supported by the National Research Foundation, Singapore under its AI Singapore Programme (AISG Award No: AISG2-RP-2021-022) and Alibaba-NTU Singapore Joint Research Institute (JRI).

References

[1] Somak Aditya, Rudra Saha, Yezhou Yang, and Chitta Baral. Spatial knowledge distillation to aid visual reasoning. In *2019 IEEE Winter Conference on Applications of Computer Vision (WACV)*, pages 227–235. IEEE, 2019.

[2] Sungsoo Ahn, Shell Xu Hu, Andreas Damianou, Neil D Lawrence, and Zhenwen Dai. Variational information distillation for knowledge transfer. In *Proceedings of the IEEE/CVF Conference on Computer Vision and Pattern Recognition*, pages 9163–9171, 2019.

[3] Qingyao Ai, Keping Bi, Cheng Luo, Jiafeng Guo, and W Bruce Croft. Unbiased learning to rank with unbiased propensity estimation. In *The 41st International ACM SIGIR Conference on Research & Development in Information Retrieval*, pages 385–394, 2018.

[4] Martin Arjovsky, Léon Bottou, Ishaan Gulrajani, and David Lopez-Paz. Invariant risk minimization. *arXiv preprint arXiv:1907.02893*, 2019.

[5] Peter C Austin. An introduction to propensity score methods for reducing the effects of confounding in observational studies. *Multivariate behavioral research*, 46(3):399–424, 2011.

[6] Steffen Bickel, Michael Brückner, and Tobias Scheffer. Discriminative learning under covariate shift. *Journal of Machine Learning Research*, 10(9), 2009.

[7] Pengguang Chen, Shu Liu, Hengshuang Zhao, and Jiaya Jia. Distilling knowledge via knowledge review. In *Proceedings of the IEEE/CVF Conference on Computer Vision and Pattern Recognition*, pages 5008–5017, 2021.

[8] Jang Hyun Cho and Bharath Hariharan. On the efficacy of knowledge distillation. In *Proceedings of the IEEE/CVF International Conference on Computer Vision*, pages 4794–4802, 2019.

[9] Corinna Cortes, Mehryar Mohri, Michael Riley, and Afshin Rostamizadeh. Sample selection bias correction theory. In *International conference on algorithmic learning theory*, pages 38–53. Springer, 2008.

[10] Jia Deng, Wei Dong, Richard Socher, Li-Jia Li, Kai Li, and Li Fei-Fei. Imagenet: A large-scale hierarchical image database. In *2009 IEEE conference on computer vision and pattern recognition*, pages 248–255. Ieee, 2009.

[11] Bin Dong, Jikai Hou, Yiping Lu, and Zhihua Zhang. Distillation $\approx$ early stopping? harvesting dark knowledge utilizing anisotropic information retrieval for overparameterized neural network. *arXiv preprint arXiv:1910.01255*, 2019.

[12] Lixin Duan, Ivor W Tsang, and Dong Xu. Domain transfer multiple kernel learning. *IEEE Transactions on Pattern Analysis and Machine Intelligence*, 34(3):465–479, 2012.

[13] Tommaso Furlanello, Zachary Lipton, Michael Tschannen, Laurent Itti, and Anima Anandkumar. Born again neural networks. In *International Conference on Machine Learning*, pages 1607–1616. PMLR, 2018.

[14] Yonatan Geifman, Guy Uziel, and Ran El-Yaniv. Bias-reduced uncertainty estimation for deep neural classifiers. *arXiv preprint arXiv:1805.08206*, 2018.

[15] Jianping Gou, Baosheng Yu, Stephen J Maybank, and Dacheng Tao. Knowledge distillation: A survey. *International Journal of Computer Vision*, 129(6):1789–1819, 2021.

[16] Kaiming He, Xiangyu Zhang, Shaoqing Ren, and Jian Sun. Deep residual learning for image recognition. In *Proceedings of the IEEE conference on computer vision and pattern recognition*, pages 770–778, 2016.

[17] Kaiming He, Xiangyu Zhang, Shaoqing Ren, and Jian Sun. Identity mappings in deep residual networks. In *European conference on computer vision*, pages 630–645. Springer, 2016.

[18] Tong He, Chunhua Shen, Zhi Tian, Dong Gong, Changming Sun, and Youliang Yan. Knowledge adaptation for efficient semantic segmentation. In *Proceedings of the IEEE/CVF Conference on Computer Vision and Pattern Recognition*, pages 578–587, 2019.

[19] Byeongho Heo, Jeesoo Kim, Sangdoo Yun, Hyojin Park, Nojun Kwak, and Jin Young Choi. A comprehensive overhaul of feature distillation. In *Proceedings of the IEEE/CVF International Conference on Computer Vision*, pages 1921–1930, 2019.

[20] Byeongho Heo, Minsik Lee, Sangdoo Yun, and Jin Young Choi. Knowledge transfer via distillation of activation boundaries formed by hidden neurons. In *Proceedings of the AAAI Conference on Artificial Intelligence*, volume 33, pages 3779–3787, 2019.

[21] Geoffrey Hinton, Oriol Vinyals, and Jeff Dean. Distilling the knowledge in a neural network. *arXiv preprint arXiv:1503.02531*, 2015.

[22] Youngkyu Hong, Seungju Han, Kwanghee Choi, Seokjun Seo, Beomsu Kim, and Buru Chang. Disentangling label distribution for long-tailed visual recognition. In *Proceedings of the IEEE/CVF conference on computer vision and pattern recognition*, pages 6626–6636, 2021.

[23] Xinting Hu, Kaihua Tang, Chunyan Miao, Xian-Sheng Hua, and Hanwang Zhang. Distilling causal effect of data in class-incremental learning. In *Proceedings of the IEEE/CVF Conference on Computer Vision and Pattern Recognition*, pages 3957–3966, 2021.

[24] Gao Huang, Zhuang Liu, Laurens Van Der Maaten, and Kilian Q Weinberger. Densely connected convolutional networks. In *Proceedings of the IEEE conference on computer vision and pattern recognition*, pages 4700–4708, 2017.

[25] Zehao Huang and Naiyan Wang. Like what you like: Knowledge distill via neuron selectivity transfer. *arXiv preprint arXiv:1707.01219*, 2017.

[26] Guido W Imbens and Donald B Rubin. *Causal inference in statistics, social, and biomedical sciences*. Cambridge University Press, 2015.

[27] Mingi Ji, Seungjae Shin, Seunghyun Hwang, Gibeom Park, and Il-Chul Moon. Refine myself by teaching myself: Feature refinement via self-knowledge distillation. In *Proceedings of the IEEE/CVF Conference on Computer Vision and Pattern Recognition*, pages 10664–10673, 2021.

[28] Xiao Jin, Baoyun Peng, Yichao Wu, Yu Liu, Jiaheng Liu, Ding Liang, Junjie Yan, and Xiaolin Hu. Knowledge distillation via route constrained optimization. In *Proceedings of the IEEE/CVF International Conference on Computer Vision*, pages 1345–1354, 2019.

[29] Bingyi Kang, Saining Xie, Marcus Rohrbach, Zhicheng Yan, Albert Gordo, Jiashi Feng, and Yannis Kalantidis. Decoupling representation and classifier for long-tailed recognition. In *International Conference on Learning Representations*, 2019.

[30] Jangho Kim, SeongUk Park, and Nojun Kwak. Paraphrasing complex network: network compression via factor transfer. In *Proceedings of the 32nd International Conference on Neural Information Processing Systems*, pages 2765–2774, 2018.

[31] Kyungyul Kim, ByeongMoon Ji, Doyoung Yoon, and Sangheum Hwang. Self-knowledge distillation with progressive refinement of targets. In *Proceedings of the IEEE/CVF International Conference on Computer Vision*, pages 6567–6576, 2021.

[32] Alex Krizhevsky, Geoffrey Hinton, et al. Learning multiple layers of features from tiny images. 2009.

[33] Solomon Kullback and Richard A Leibler. On information and sufficiency. *The annals of mathematical statistics*, 22(1):79–86, 1951.

[34] Quanquan Li, Shengying Jin, and Junjie Yan. Mimicking very efficient network for object detection. In *Proceedings of the ieee conference on computer vision and pattern recognition*, pages 6356–6364, 2017.

[35] Xiaojie Li, Jianlong Wu, Hongyu Fang, Yue Liao, Fei Wang, and Chen Qian. Local correlation consistency for knowledge distillation. In *European Conference on Computer Vision*, pages 18–33. Springer, 2020.

[36] Zhizhong Li and Derek Hoiem. Learning without forgetting. *IEEE transactions on pattern analysis and machine intelligence*, 40(12):2935–2947, 2017.

[37] Roderick JA Little and Donald B Rubin. *Statistical analysis with missing data*, volume 793. John Wiley & Sons, 2019.

[38] Yifan Liu, Ke Chen, Chris Liu, Zengchang Qin, Zhenbo Luo, and Jingdong Wang. Structured knowledge distillation for semantic segmentation. In *Proceedings of the IEEE/CVF Conference on Computer Vision and Pattern Recognition*, pages 2604–2613, 2019.

[39] Zelun Luo, Jun-Ting Hsieh, Lu Jiang, Juan Carlos Niebles, and Li Fei-Fei. Graph distillation for action detection with privileged modalities. In *Proceedings of the European Conference on Computer Vision (ECCV)*, pages 166–183, 2018.

[40] Ningning Ma, Xiangyu Zhang, Hai-Tao Zheng, and Jian Sun. Shufflenet v2: Practical guidelines for efficient cnn architecture design. In *Proceedings of the European conference on computer vision (ECCV)*, pages 116–131, 2018.

[41] Aditya K Menon, Ankit Singh Rawat, Sashank Reddi, Seungyeon Kim, and Sanjiv Kumar. A statistical perspective on distillation. In *International Conference on Machine Learning*, pages 7632–7642. PMLR, 2021.

[42] Aditya Krishna Menon, Sadeep Jayasumana, Ankit Singh Rawat, Himanshu Jain, Andreas Veit, and Sanjiv Kumar. Long-tail learning via logit adjustment. *arXiv preprint arXiv:2007.07314*, 2020.

[43] Seyed Iman Mirzadeh, Mehrdad Farajtabar, Ang Li, Nir Levine, Akihiro Matsukawa, and Hassan Ghasemzadeh. Improved knowledge distillation via teacher assistant. In *Proceedings of the AAAI Conference on Artificial Intelligence*, volume 34, pages 5191–5198, 2020.

[44] Ravi Teja Mullapudi, Steven Chen, Keyi Zhang, Deva Ramanan, and Kayvon Fatahalian. Online model distillation for efficient video inference. In *Proceedings of the IEEE/CVF International Conference on Computer Vision*, pages 3573–3582, 2019.

[45] Rafael Müller, Simon Kornblith, and Geoffrey Hinton. When does label smoothing help? *arXiv preprint arXiv:1906.02629*, 2019.

[46] Jonghwan Mun, Kimin Lee, Jinwoo Shin, and Bohyung Han. Learning to specialize with knowledge distillation for visual question answering. In *NeurIPS*, pages 8092–8102, 2018.

[47] Mahdi Pakdaman Naeini, Gregory Cooper, and Milos Hauskrecht. Obtaining well calibrated probabilities using bayesian binning. In *Twenty-Ninth AAAI Conference on Artificial Intelligence*, 2015.

[48] Yulei Niu and Hanwang Zhang. Introspective distillation for robust question answering. *Advances in Neural Information Processing Systems*, 34:16292–16304, 2021.

[49] Boxiao Pan, Haoye Cai, De-An Huang, Kuan-Hui Lee, Adrien Gaidon, Ehsan Adeli, and Juan Carlos Niebles. Spatio-temporal graph for video captioning with knowledge distillation. In *Proceedings of the IEEE/CVF Conference on Computer Vision and Pattern Recognition*, pages 10870–10879, 2020.

[50] Wonpyo Park, Dongju Kim, Yan Lu, and Minsu Cho. Relational knowledge distillation. In *Proceedings of the IEEE/CVF Conference on Computer Vision and Pattern Recognition*, pages 3967–3976, 2019.

[51] Nikolaos Passalis and Anastasios Tefas. Learning deep representations with probabilistic knowledge transfer. In *Proceedings of the European Conference on Computer Vision (ECCV)*, pages 268–284, 2018.

[52] Baoyun Peng, Xiao Jin, Jiaheng Liu, Dongsheng Li, Yichao Wu, Yu Liu, Shunfeng Zhou, and Zhaoning Zhang. Correlation congruence for knowledge distillation. In *Proceedings of the IEEE/CVF International Conference on Computer Vision*, pages 5007–5016, 2019.

[53] Zhimao Peng, Zechao Li, Junge Zhang, Yan Li, Guo-Jun Qi, and Jinhui Tang. Few-shot image recognition with knowledge transfer. In *Proceedings of the IEEE/CVF International Conference on Computer Vision*, pages 441–449, 2019.

[54] Adriana Romero, Nicolas Ballas, Samira Ebrahimi Kahou, Antoine Chassang, Carlo Gatta, and Yoshua Bengio. Fitnets: Hints for thin deep nets. *arXiv preprint arXiv:1412.6550*, 2014.

[55] Paul R Rosenbaum and Donald B Rubin. The central role of the propensity score in observational studies for causal effects. *Biometrika*, 70(1):41–55, 1983.

[56] Mark Sandler, Andrew Howard, Menglong Zhu, Andrey Zhmoginov, and Liang-Chieh Chen. Mobilenetv2: Inverted residuals and linear bottlenecks. In *Proceedings of the IEEE conference on computer vision and pattern recognition*, pages 4510–4520, 2018.

[57] Tobias Schnabel, Adith Swaminathan, Ashudeep Singh, Navin Chandak, and Thorsten Joachims. Recommendations as treatments: Debiasing learning and evaluation. In *international conference on machine learning*, pages 1670–1679. PMLR, 2016.

[58] Zhiqiang Shen, Zechun Liu, Dejia Xu, Zitian Chen, Kwang-Ting Cheng, and Marios Savvides. Is label smoothing truly incompatible with knowledge distillation: An empirical study. In *International Conference on Learning Representations*, 2020.

[59] Konstantin Shmelkov, Cordelia Schmid, and Karteek Alahari. Incremental learning of object detectors without catastrophic forgetting. In *Proceedings of the IEEE international conference on computer vision*, pages 3400–3409, 2017.

[60] Karen Simonyan and Andrew Zisserman. Very deep convolutional networks for large-scale image recognition. *arXiv preprint arXiv:1409.1556*, 2014.

[61] Wonchul Son, Jaemin Na, Junyong Choi, and Wonjun Hwang. Densely guided knowledge distillation using multiple teacher assistants. In *Proceedings of the IEEE/CVF International Conference on Computer Vision*, pages 9395–9404, 2021.

[62] Masashi Sugiyama and Motoaki Kawanabe. *Machine learning in non-stationary environments: Introduction to covariate shift adaptation*. MIT press, 2012.

[63] Ben Tan, Yu Zhang, Sinno Pan, and Qiang Yang. Distant domain transfer learning. In *Proceedings of the AAAI conference on artificial intelligence*, volume 31, 2017.

[64] Hongchen Tan, Xiuping Liu, Meng Liu, Baocai Yin, and Xin Li. Kt-gan: knowledge-transfer generative adversarial network for text-to-image synthesis. *IEEE Transactions on Image Processing*, 30:1275–1290, 2020.

[65] Kaihua Tang, Jianqiang Huang, and Hanwang Zhang. Long-tailed classification by keeping the good and removing the bad momentum causal effect. *Advances in Neural Information Processing Systems*, 33:1513–1524, 2020.

[66] Yonglong Tian, Dilip Krishnan, and Phillip Isola. Contrastive representation distillation. *arXiv preprint arXiv:1910.10699*, 2019.

[67] Antonio Torralba and Alexei A Efros. Unbiased look at dataset bias. In *CVPR 2011*, pages 1521–1528. IEEE, 2011.

[68] Frederick Tung and Greg Mori. Similarity-preserving knowledge distillation. In *Proceedings of the IEEE/CVF International Conference on Computer Vision*, pages 1365–1374, 2019.

[69] Tan Wang, Zhongqi Yue, Jianqiang Huang, Qianru Sun, and Hanwang Zhang. Self-supervised learning disentangled group representation as feature. *arXiv preprint arXiv:2110.15255*, 2021.

[70] Tao Wang, Li Yuan, Xiaopeng Zhang, and Jiashi Feng. Distilling object detectors with fine-grained feature imitation. In *Proceedings of the IEEE/CVF Conference on Computer Vision and Pattern Recognition*, pages 4933–4942, 2019.

[71] Xudong Wang, Long Lian, Zhongqi Miao, Ziwei Liu, and Stella X Yu. Long-tailed recognition by routing diverse distribution-aware experts. *arXiv preprint arXiv:2010.01809*, 2020.

[72] Yixin Wang, Dawen Liang, Laurent Charlin, and David M Blei. The deconfounded recommender: A causal inference approach to recommendation. *arXiv preprint arXiv:1808.06581*, 2018.

[73] Saining Xie, Ross Girshick, Piotr Dollár, Zhuowen Tu, and Kaiming He. Aggregated residual transformations for deep neural networks. In *Proceedings of the IEEE conference on computer vision and pattern recognition*, pages 1492–1500, 2017.

[74] Guodong Xu, Ziwei Liu, Xiaoxiao Li, and Chen Change Loy. Knowledge distillation meets self-supervision. In *European Conference on Computer Vision*, pages 588–604. Springer, 2020.

[75] Chenglin Yang, Lingxi Xie, Chi Su, and Alan L Yuille. Snapshot distillation: Teacher-student optimization in one generation. In *Proceedings of the IEEE/CVF Conference on Computer Vision and Pattern Recognition*, pages 2859–2868, 2019.

[76] Junho Yim, Donggyu Joo, Jihoon Bae, and Junmo Kim. A gift from knowledge distillation: Fast optimization, network minimization and transfer learning. In *Proceedings of the IEEE Conference on Computer Vision and Pattern Recognition*, pages 4133–4141, 2017.

[77] Li Yuan, Francis EH Tay, Guilin Li, Tao Wang, and Jiashi Feng. Revisiting knowledge distillation via label smoothing regularization. In *Proceedings of the IEEE/CVF Conference on Computer Vision and Pattern Recognition*, pages 3903–3911, 2020.

[78] Sukmin Yun, Jongjin Park, Kimin Lee, and Jinwoo Shin. Regularizing class-wise predictions via self-knowledge distillation. In *Proceedings of the IEEE/CVF conference on computer vision and pattern recognition*, pages 13876–13885, 2020.

[79] Sergey Zagoruyko and Nikos Komodakis. Paying more attention to attention: Improving the performance of convolutional neural networks via attention transfer. *arXiv preprint arXiv:1612.03928*, 2016.

[80] Sergey Zagoruyko and Nikos Komodakis. Wide residual networks. *arXiv preprint arXiv:1605.07146*, 2016.

[81] Linfeng Zhang, Chenglong Bao, and Kaisheng Ma. Self-distillation: Towards efficient and compact neural networks. *IEEE Transactions on Pattern Analysis and Machine Intelligence*, 2021.

[82] Linfeng Zhang, Jiebo Song, Anni Gao, Jingwei Chen, Chenglong Bao, and Kaisheng Ma. Be your own teacher: Improve the performance of convolutional neural networks via self distillation. In *Proceedings of the IEEE/CVF International Conference on Computer Vision*, pages 3713–3722, 2019.

[83] Xiangyu Zhang, Xinyu Zhou, Mengxiao Lin, and Jian Sun. Shufflenet: An extremely efficient convolutional neural network for mobile devices. In *Proceedings of the IEEE conference on computer vision and pattern recognition*, pages 6848–6856, 2018.

[84] Ziqi Zhang, Yaya Shi, Chunfeng Yuan, Bing Li, Peijin Wang, Weiming Hu, and Zheng-Jun Zha. Object relational graph with teacher-recommended learning for video captioning. In *Proceedings of the IEEE/CVF conference on computer vision and pattern recognition*, pages 13278–13288, 2020.

[85] Helong Zhou, Liangchen Song, Jiajie Chen, Ye Zhou, Guoli Wang, Junsong Yuan, and Qian Zhang. Rethinking soft labels for knowledge distillation: A bias-variance tradeoff perspective. *arXiv preprint arXiv:2102.00650*, 2021.

Checklist

1. For all authors...
   (a) Do the main claims made in the abstract and introduction accurately reflect the paper's contributions and scope? [Yes]
   (b) Did you describe the limitations of your work? [Yes] See Section 4.2
   (c) Did you discuss any potential negative societal impacts of your work? [Yes] To the best of our knowledge, as our work is purely an algorithm for knowledge distillation, we haven't found any negative societal impact.

(d) Have you read the ethics review guidelines and ensured that your paper conforms to them? [Yes]

2. If you are including theoretical results...
   (a) Did you state the full set of assumptions of all theoretical results? [N/A]
   (b) Did you include complete proofs of all theoretical results? [N/A]
3. If you ran experiments...
   (a) Did you include the code, data, and instructions needed to reproduce the main experimental results (either in the supplemental material or as a URL)? [Yes] Please refer to the supplemental material.
   (b) Did you specify all the training details (e.g., data splits, hyperparameters, how they were chosen)? [Yes] The details are in Section 5.
   (c) Did you report error bars (e.g., with respect to the random seed after running experiments multiple times)? [Yes] We run the experiments with five different random seeds.
   (d) Did you include the total amount of compute and the type of resources used (e.g., type of GPUs, internal cluster, or cloud provider)? [Yes] See Appendix.
4. If you are using existing assets (e.g., code, data, models) or curating/releasing new assets...
   (a) If your work uses existing assets, did you cite the creators? [Yes]
   (b) Did you mention the license of the assets? [Yes] See Appendix.
   (c) Did you include any new assets either in the supplemental material or as a URL? [Yes]
   (d) Did you discuss whether and how consent was obtained from people whose data you're using/curating? [Yes] All the used existing assets are open-sourced for research.
   (e) Did you discuss whether the data you are using/curating contains personally identifiable information or offensive content? [Yes] The benchmark dataset does not contain personally identifiable information or offensive content.
5. If you used crowdsourcing or conducted research with human subjects...
   (a) Did you include the full text of instructions given to participants and screenshots, if applicable? [N/A]
   (b) Did you describe any potential participant risks, with links to Institutional Review Board (IRB) approvals, if applicable? [N/A]
   (c) Did you include the estimated hourly wage paid to participants and the total amount spent on participant compensation? [N/A]

Appendix

A Experimental Settings

A.1 Two-stage Distillation

Implementation. We follow the training details of Tian *et al.* [66] for CIFAR-100 and Zhou *et al.* [85] for ImageNet. Specifically, for CIFAR-100, we set the mini-batch size as 64 and an initial learning rate as 0.05. We train the model for 240 epochs. The learning rate is decayed by 10 every 30 epochs after 150 epochs. We initialize the learning rate as 0.01 for MobileNetV2, ShuffleNetV1 and ShuffleNetV2, and as 0.05 for other models. The experiments are conducted using one NVIDIA TITAN RTX GPU. For ImageNet, we train the model for 100 epochs. We set the mini-batch size as 256, an initial learning rate as 0.1, and decay it by 10 every 30 epochs. The experiments are conducted using four Tesla V100 GPUs.

Architectures. We follow Tian *et al.* [66] for the choice of network architectures. Specifically, "WRN-d-w" denotes Wide Residual Network (WRN) [80] with depth d and width factor w. "resnet-d" represents cifar-style ResNet [16] with 3 groups of basic blocks, each with 16, 32, and 64 channels respectively. For example, resnet8x4 and resnet32x4 represent a 4 times wider network, *i.e.*, with 64, 128, and 256 channels respectively. "ResNet-d" represents the ImageNet-style ResNet with Bottleneck blocks and more channels. MobileNetV2 [56] has a width multiplier of 0.5. "vgg" denotes VGGNet [60] that is adapted from its original ImageNet counterpart. "ShuffleNetV1" [83], "ShuffleNetV2" [40] are adapted with input size as 32x32.

A.2 One-stage Self-Distillation

Implementation. We follow all the training details of PS-KD [31]. The standard data argumentation schemes are 32x32 random crop after padding with 4 pixels and random horizontal flip. The networks are trained for 300 epochs using SGD with a momentum of 0.9. The learning rate is decayed by 10 at 150 and 225 epochs. We set the mini-batch size as 128, an initial learning rate as 0.1, and a weight decay as 0.0005. The experiments are conducted using four Tesla V100 GPUs.

Metrics. Besides top-1 and top-5 accuracies, we follow Kim *et al.* [31] and report Expected calibration error (ECE) and Area under risk-coverage curve (AURC) for evaluation. Expected calibration error (ECE) [47] is used to evaluate the confidence calibration performance of models, *i.e.*, the expected gap between accuracy and confidence. Specifically, the samples are partitioned by confidence into M bins $B_1, \cdots, B_M$. The m-th bin B_m contains samples with confidence within $[\frac{m-1}{M}, \frac{m}{M}]$. For N samples, ECE is formulated as:

$$\text{BCE} = \frac{1}{N} \sum_{m=1}^{M} |B_m| \times |\text{Acc}(B_m) - \text{Conf}(B_m)|,$$

where $\text{Acc}(B_m)$ denotes the accuracy of samples in B_m, and $\text{Conf}(B_m)$ denotes the average confidence of samples in B_m. A lower BCE indicates a well-calibrated model.

Area under risk-coverage curve (AURC) [14] measures how well predictions are ordered by confidence values. Specifically, we can determine a threshold for classification, where only samples with confidence higher than the threshold are accepted. After that, we can obtain the proportion of covered samples to the whole dataset, *i.e.*, coverage, and define the risk as the error rate computed by using the covered samples. AURC is defined as the area under the risk-coverage curve. A lower AURC indicates that the correct and incorrect predictions are well-separable by confidence values.

A.3 License of Assets

We reimplemented WSLD[2] and SSKD[3] based on their open-resourced codes. Both WSLD and SSKD did not mention the license in their open-resourced codes.

B Additional Results

B.1 Architecture styles

Due to page limitation, we did not include all the results of different architecture styles on CIFAR-100 in the main paper. We provide additional results in Table 8. Results show that our IPWD achieves competitive performances and outperforms KD by large margins.

B.2 Feature-based Methods

Note that our proposed IPWD is a logit-based distillation method. An interesting question is whether the reweighting strategy can work with feature-based distillation methods. We select ReviewKD as an example, which is a recent representative feature-based distillation method. As shown in Figure 9, the gap between ReviewKD+IPWD and ReviewKD is very marginal, which indicates that IPWD cannot promote feature-based distillation. The possible reasons are two-fold. First, the logit knowledge of label y is long-tailed but the representation knowledge of sample x may be relatively balanced. Second, as pointed out by Kang *et al.* [29], "data imbalance might not be an issue in learning high-quality representations" for long-tailed classification, which implies that the reweighting strategy is not compatible at feature level.

B.3 Long-tailed Methods for KD

Note that Figure 1 shows that there seems long-tailed property of teacher predictions. An interesting question is whether it could be fixed by techniques for long-tailed classification. We take LA [42]

[2] `https://github.com/bellymonster/Weighted-Soft-Label-Distillation`

[3] `https://github.com/xuguodong03/SSKD`

Table 8: Top-1 accuracy of student networks on CIFAR-100 test set for the two-stage distillation setting. * denotes our reproduced results using the same teacher model.

	Same architecture style		Different architecture style	
Teacher Student	WRN-40-2 WRN-16-2	resnet110 resnet20	resnet32x4 ShuffleNetV2	vgg13 MobileNetV2
Teacher	75.61	74.31	79.42	74.64
Student	73.26	69.06	71.82	64.60
FitNet [54]	73.58	68.99	73.54	64.14
AT [79]	74.08	70.22	72.73	59.40
SP [68]	73.83	70.04	74.56	66.30
CC [52]	73.56	69.48	71.29	64.86
VID [2]	74.11	70.16	73.40	65.56
RKD [50]	73.35	69.25	73.21	64.52
PKT [51]	74.54	70.25	74.69	67.13
AB [20]	72.50	69.53	74.31	66.06
FT [30]	73.25	70.22	72.50	61.78
NST [25]	73.68	69.53	74.68	58.16
KD [21]	74.92	70.67	74.45	67.37
CRD [66]	75.48	**71.46**	75.65	69.73
WSLD* [85]	75.63	71.20	75.55	68.50
IPWD	**75.83**	71.22	**76.61**	**69.81**

Table 9: ReviewKD with our IPWD reweighting strategy on feature level.

Teacher Student	WRN-40-2 WRN-16-2	resnet56 resnet20	resnet110 resnet32	resnet32x4 ShuffleV2	WRN-40-2 ShuffleV1
ReviewKD	76.12	**71.89**	**73.89**	**77.78**	**77.14**
ReviewKD + IPWD	**76.25**	71.51	73.79	77.74	77.06

as the recent representative technique for long-tailed classification. LA proposed a logit adjusted softmax cross-entropy loss by applying a class prior to each logit. LA does not require extra modules (compared to TDE [65]), post-hoc logit adjustment (compared to LADE [22]), or ensemble of multiple models (compared to RIDE [71]).

Following LA, we applied the class prior to the student output when calculating the KL divergence distillation loss. We found that KD+LA underperforms KD by averagely 0.5% on CIFAR-100. The possible reason is that the introduced prior indirectly breaks the teacher's knowledge for each training sample, which hurts the effectiveness of distillation. These results indicate that logit-adjust-based long-tailed techniques are not applicable to the issue of KD.

B.4 Ablation Studies

We have conducted ablation studies on the components of our proposed IPWD. In the appendix, we further provide ablation studies on the technical designs.

We take two-stage distillation on CIFAR-100 as an example. Recall that the sample weights are estimated based on the two types of student's outputs, KD-trained output y^{kd} from the student's original head and CLS-trained output y^{cls} from the student's extra head. We further conduct ablations on the selection of two outputs.

For CE-aware output y^{cls}, an straightforward alternative is using an extra model that has the same architecture as student with totally different parameters. This extra model is trained using the cross-entropy classification loss. In other words, the difference is whether the visual backbone is shared for the two outputs. We denote this alternative as IPWD*. Table 10 shows the comparison. Overall, IPWD* achieves competitive results compared to IPWD. However, training an extra model leads to more memory and time cost. Therefore, our design that takes an extra head is both effective and efficient.

Table 10: Ablation study of CE-aware output on CIFAR-100. * denotes that the CE-aware output is obtained from an extra student model.

Teacher Student	resnet110 resnet32	resnet32x4 resnet8x4	resnet32x4 ShuffleV1	resnet32x4 ShuffleV2
Teacher	74.31	79.42	79.42	79.42
Student	71.14	72.50	70.50	71.82
IPWD*	73.64	75.88	75.98	76.83
IPWD	73.91	76.03	76.03	76.61

Table 11: Ablation study of KD-aware output on CIFAR-100. † denotes that the KD-aware output is obtained from another extra head trained only with the original distillation loss.

Teacher Student	resnet110 resnet32	resnet32x4 resnet8x4	resnet32x4 ShuffleV1	resnet32x4 ShuffleV2
Teacher	74.31	79.42	79.42	79.42
Student	71.14	72.50	70.50	71.82
IPWD†	73.56	75.88	75.93	76.44
IPWD	73.91	76.03	76.03	76.61

For KD-trained output y^{kd}, an straightforward alternative is using an extra distillation head like the classification head. Different from the original head of the student, the distillation head is trained only using the distillation loss, which simply mimics the teacher's output without ground-truth annotations. We denote this alternative as IPWD†. Table 11 shows the comparison. Overall, IPWD† slightly underperforms IPWD with different four architectures. The reason is that the extra distillation head only learns from the teacher model, which is sensitive to the teacher's performance and weights hard samples more. These two ablation studies further verify the effectiveness of our techinical designs.